

## Entanglement complexity of semiflexible lattice polygons

This article has been downloaded from IOPscience. Please scroll down to see the full text article.

2005 J. Phys. A: Math. Gen. 38 L795

(<http://iopscience.iop.org/0305-4470/38/47/L02>)

View [the table of contents for this issue](#), or go to the [journal homepage](#) for more

Download details:

IP Address: 171.66.16.94

The article was downloaded on 03/06/2010 at 04:03

Please note that [terms and conditions apply](#).

## LETTER TO THE EDITOR

## Entanglement complexity of semiflexible lattice polygons

E Orlandini<sup>1</sup>, M C Tesi<sup>2</sup> and S G Whittington<sup>3</sup>

<sup>1</sup> Dipartimento di Fisica and Sezione INFN, Università di Padova, Padova, Italy

<sup>2</sup> Dipartimento di Matematica, Università di Bologna, Bologna, Italy

<sup>3</sup> Department of Chemistry, University of Toronto, Toronto, M5S 3H6, Canada

Received 3 October 2005

Published 9 November 2005

Online at [stacks.iop.org/JPhysA/38/L795](http://stacks.iop.org/JPhysA/38/L795)

### Abstract

We use Monte Carlo methods to study knotting in polygons on the simple cubic lattice with a stiffness fugacity. We investigate how the knot probability depends on stiffness and how the relative frequency of trefoils and figure eight knots changes as the stiffness changes. In addition, we examine the effect of stiffness on the writhe of the polygons.

PACS numbers: 05.50.+q, 05.10.Ln, 82.35.Lr

(Some figures in this article are in colour only in the electronic version)

Long linear polymers in dilute solution can be self-entangled and, if a ring closure occurs, these entanglements can be captured as a knot in the ensuing ring polymer. This phenomenon has been widely studied, partly because of its relevance to molecular biology where the presence of knots in circular DNA can give information about the mechanism of action of enzymes, such as topoisomerases and recombinases [1–3]. Knots and entanglements also affect physical properties of polymers [4].

Random knotting has been studied seriously for the last 20 years in a variety of models of ring polymers. One popular model is polygons on the simple cubic lattice  $Z^3$  or on other three-dimensional lattices. It is known rigorously [5, 6] that the probability that a lattice polygon is unknotted goes to zero exponentially rapidly as the number of edges ( $n$ ) in the polygon goes to infinity. Similar results are known [7] for some off-lattice models. These theorems do not say much about knot probabilities when  $n$  is finite but there are many Monte Carlo studies of this question [8–10]. Some of these [9, 10] have looked at the relative probability of forming different knot types.

Since different polymer molecules have different flexibilities, it is natural to ask how the knot probability depends on the flexibility. Since the number of right angles (between adjacent edges) in a polygon are related to flexibility, we associate a number  $c_i$  to the  $i$ th vertex,  $i = 1, 2, \dots, n$ , where  $c_i$  is 1 if the two edges meeting at vertex  $i$  are at right

angles and zero otherwise. Then, we define the curvature of the polygon as  $k = \sum_i c_i$ . Let  $p_n(k)$  be the number of  $n$ -edge polygons with curvature  $k$ . Define the partition function as

$$Z_n(\gamma) = \sum_k p_n(k) e^{\gamma k}, \quad (1)$$

where  $\gamma$  is the curvature fugacity. It is known [11] that the limit

$$F(\gamma) = \lim_{n \rightarrow \infty} n^{-1} \log Z_n(\gamma) \quad (2)$$

exists. If we define  $p_n^0(k)$  to be the number of  $n$ -edge unknotted polygons with curvature  $k$  then the corresponding partition function is

$$Z_n^0(\gamma) = \sum_k p_n^0(k) e^{\gamma k} \quad (3)$$

and the limit

$$F^0(\gamma) = \lim_{n \rightarrow \infty} n^{-1} \log Z_n^0(\gamma) \quad (4)$$

exists [11]. The probability that a polygon is unknotted at curvature fugacity  $\gamma$  is

$$P_n^0(\gamma) = \frac{Z_n^0(\gamma)}{Z_n(\gamma)} = \exp(-(F(\gamma) - F^0(\gamma))n + o(n)) \quad (5)$$

and it is known [11] that  $F^0(\gamma) < F(\gamma)$  for all finite  $\gamma$ . That is, unknotted polygons are exponentially rare for every finite curvature fugacity. A natural question which follows from this is how  $F(\gamma) - F^0(\gamma)$  depends on  $\gamma$ . For instance, is  $F(\gamma) - F^0(\gamma)$  monotone in  $\gamma$ ? Such questions are beyond the reach of current rigorous approaches and in this letter we shall investigate this kind of question using Monte Carlo methods.

Lattice polygons with a fixed number of vertices can be sampled efficiently by Monte Carlo methods based on a two-point pivot algorithm [12]. Although this algorithm works well for  $\gamma = 0$ , at large  $\gamma$  quasi-ergodic problems can occur. To mitigate this problem, we have combined the pivot algorithm with the multiple Markov chain algorithm [13]. The idea is to run a set of Markov chains in parallel (at a fixed set of  $\gamma$  values) and to swap configurations between the individual Markov chains. For details see [14, 15]. Simulations have been carried out by considering up to 17 Markov chains in parallel and configurations have been sampled every  $m$ -attempted pivot moves. The value of  $m$  increases with the number of edges ( $n$ ) in the polygon and it ranges from 100 (for  $n = 400$ ) up to 7200 (for  $n = 3200$ ). The data were analyzed by using standard techniques to find autocorrelation times and statistical confidence intervals [16].

Once a polygon has been generated we need to determine if it is knotted or unknotted. We do this by computing the value of the Alexander polynomial  $\Delta(t)$  at  $t = -1$  [8, 17]. If  $|\Delta(-1)| \neq 1$  then the polygon is a knot. Otherwise we assume that it is the unknot. This procedure will miss some knots but we do not expect this to be a serious problem at the values of  $n$  which we consider. When  $|\Delta(-1)| \neq 1$ , we know that the polygon is knotted but different knots (e.g.,  $4_1$  and  $5_1$ ) can have the same value of  $|\Delta(-1)|$ . To help to distinguish pairs of knots, we have also computed  $|\Delta(-2)|$ . In fact, the Alexander polynomial itself is not a perfect invariant and is unable to distinguish every knot type. For instance, the prime knot  $8_{11}$  has the same Alexander polynomial as the composite knot  $3_1\#6_1$  and  $8_{15}$  has the same Alexander polynomial as  $3_1\#7_2$ .

The mean curvature  $\langle k \rangle$  should be an increasing function of  $\gamma$  and we show the  $\gamma$  dependence of  $\langle k \rangle/n$  for several values of  $n$  in figure 1. Clearly,  $\langle k \rangle/n$  approaches  $\lim_{n \rightarrow \infty} \langle k \rangle/n \equiv \rho(\gamma)$  rapidly as  $n \rightarrow \infty$ , and we call  $\rho(\gamma)$  the limiting density of right angles. Clearly,  $0 \leq \rho(\gamma) \leq 1$  and  $\rho(\gamma)$  approaches zero monotonically as  $\gamma \rightarrow -\infty$ .

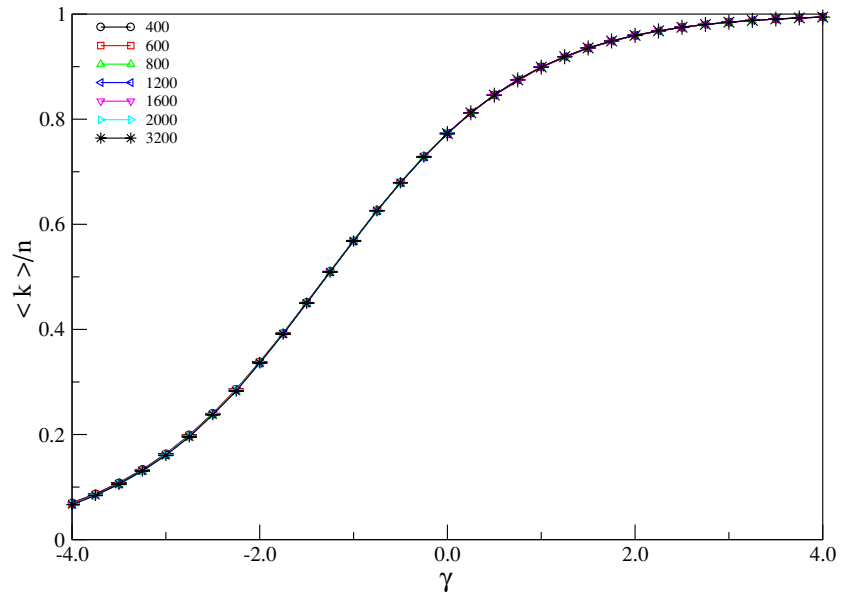


**Figure 1.** The  $\gamma$  dependence of the mean curvature density,  $\langle k \rangle/n$  for different values of  $n$ .

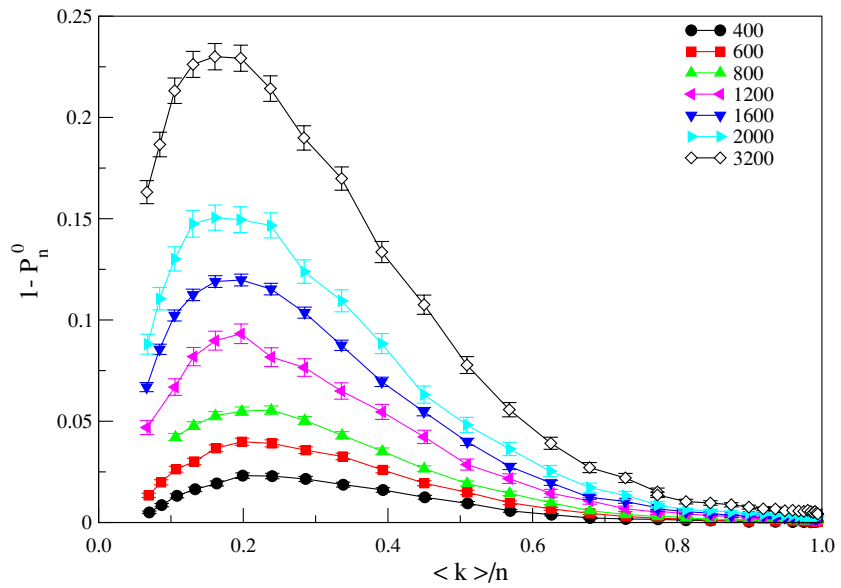


**Figure 2.** The knot probability  $1 - P_n^0$  as a function of  $\langle k \rangle/n$  for various values of  $n$ . The error bars represent one standard deviation.

The density of right angles in a polygon when  $\gamma = 0$  (i.e., when the polygons are uniformly weighted) is roughly  $\rho(0) \approx 0.77$ .

In figure 2, we show the knot probability,  $1 - P_n^0(\gamma)$ , as a function of  $\langle k \rangle/n$  for various values of  $n$ . For each value of  $n$ , the knot probability goes through a maximum at approximately  $\langle k \rangle/n \approx 0.2$ , which corresponds to  $\gamma \approx -3$ . There are two interesting things to note. First, the

values of  $1 - P_n^0(\gamma)$  are quite high at this value of  $\langle k \rangle/n$  compared to the values at  $\langle k \rangle/n \approx 0.77$  (corresponding to  $\gamma = 0$ ). Second,  $\gamma = -3$  corresponds to a rather stiff polygon with a relatively low density of right angles. At first sight this seems counter-intuitive, since one might expect knots to be less common in such stiff polygons. We believe that this increase in the knot probability can be understood by the following argument. Consider polygons with  $n$  edges with their natural density of right angles,  $\langle k \rangle/n \approx \rho(0) \approx 0.77$ . Their knot probability  $1 - P_n^0(0) \equiv P_n(0)$  is an increasing function of  $n$ , going to unity as  $n \rightarrow \infty$ . We define a *U-turn* to be a sequence of three edges  $e_1, e_2$  and  $e_3$ , such that  $e_2$  is perpendicular to  $e_1$  and  $e_3$  is the reverse of  $e_1$ . We write  $u$  for the number of U-turns and  $\lambda = \lim_{n \rightarrow \infty} \langle u \rangle/n$ . The density of U-turns at  $\gamma = 0$  is approximately 0.42. Consider now a fixed  $\gamma = \tilde{\gamma} < 0$ . At this value of  $\gamma$ , the density of right angles is  $\langle k \rangle/n \approx \rho(\tilde{\gamma})$  and the density of U-turns is  $\langle u \rangle/n \approx \lambda(\tilde{\gamma})$ . If we remove  $n(\lambda(0) - \lambda(\tilde{\gamma}))$  U-turns from typical uniformly weighted polygons with  $n$  edges, we decrease the number of edges by  $2n(\lambda(0) - \lambda(\tilde{\gamma}))$  obtaining polygons with

$$\tilde{n} = n(1 - 2\lambda(0) + 2\lambda(\tilde{\gamma})) \quad (6)$$

edges. The operation of removing U-turns does not change the knot type. Consequently, we expect the knot probability for polygons with  $n$  edges and zero curvature fugacity (i.e., with the natural density of right angles) to be comparable to the knot probability of polygons with  $\tilde{n}$  edges and curvature fugacity  $\tilde{\gamma}$ . Since  $\tilde{n} < n$  and  $P_n(0)$  is an increasing function of  $n$ , we expect that

$$P_n(0) \approx P_{\tilde{n}}(\tilde{\gamma}) > P_{\tilde{n}}(0). \quad (7)$$

Consequently, at fixed  $n$  the knot probability should increase as  $\gamma$  decreases, and therefore, as the density of right angles decreases. Of course, as  $\langle k \rangle/n \rightarrow 0$  eventually the polygon approaches a rectangle and the knot probability goes to zero. This argument roughly explains the general features seen in figure 2.

One might expect the distribution of knot types to change as  $\gamma$  changes. It is well known from numerical work that the knot type distribution depends on  $n$  [9]. For instance, the probability that the knot type of a polygon is  $3_1$  (a trefoil) first increases as  $n$  increases, and then decreases exponentially rapidly for large  $n$ . The same is true for more complicated knots but the location of the maximum in the probability is at larger values of  $n$  for more complex knots. For instance, the maximum is at larger  $n$  for  $4_1$  than for  $3_1$ . The ratio  $(P_{4_1}/P_{3_1})$  of probabilities that the knot is  $4_1$  and  $3_1$  is shown in figure 3 as a function of  $\langle k \rangle/n$  for various values of  $n$ . For the range of values of  $\langle k \rangle/n$  investigated this probability decreases as the density of right angles increases. This can be understood by an argument similar to that given above. The knot distribution at some  $\tilde{\gamma} < 0$  (but not too negative) and length  $\tilde{n}$  should be roughly the distribution at  $\gamma = 0$  and length  $n$ , where  $\tilde{n}$  and  $n$  are related by (6). For the values of  $n$  with which we are concerned the ratio  $P_{4_1}/P_{3_1}$  increases with increasing  $n$  at  $\gamma = 0$  so, at fixed  $n$ , we expect this value to be higher for  $\gamma = \tilde{\gamma} < 0$  than for  $\gamma = 0$ .

Polygons can also experience geometrical entanglement as well as topological entanglement. This can be conveniently characterized by the *writhe* ( $Wr$ ) of the polygon. We have also investigated how the writhe depends on the density of right angles for various values of  $n$ . Rigorous bounds indicate that, for all  $\gamma$ , the expectation of the absolute value of the writhe increases as least as rapidly as  $n^{1/2}$  [18, 19] and there is numerical evidence that for  $\gamma = 0$

$$\langle |Wr| \rangle \sim n^\theta \quad (8)$$

with  $\theta$  being very close to  $1/2$  [18]. In figure 4, we plot  $\langle |Wr| \rangle/n^{1/2}$  against  $\langle k \rangle/n$  and we see that the data for different values of  $n$  collapse quite well onto a single curve, suggesting that (8) is satisfied with  $\theta \approx 1/2$  for  $\gamma \neq 0$ .

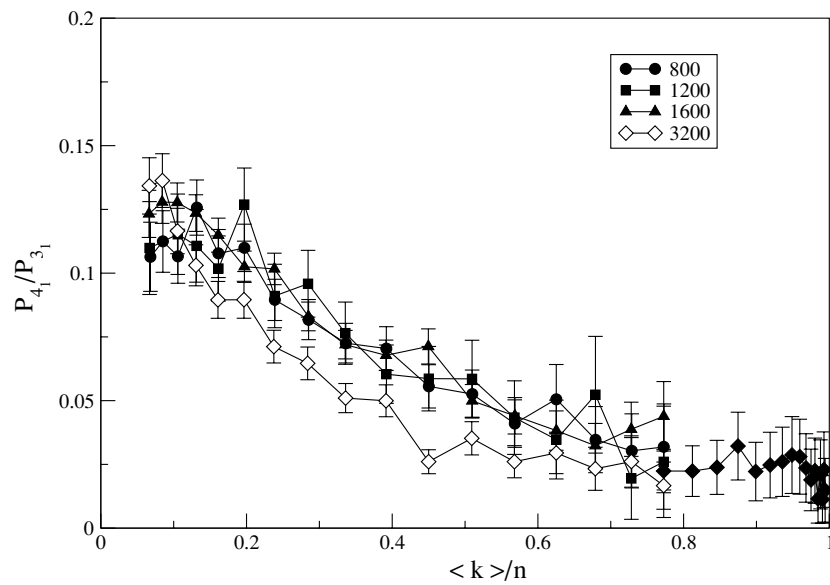


**Figure 3.** The ratio  $P_{4_1}/P_{3_1}$  of probabilities that the knot is  $4_1$  and  $3_1$  as a function of  $\langle k \rangle/n$  for different values of  $n$ .

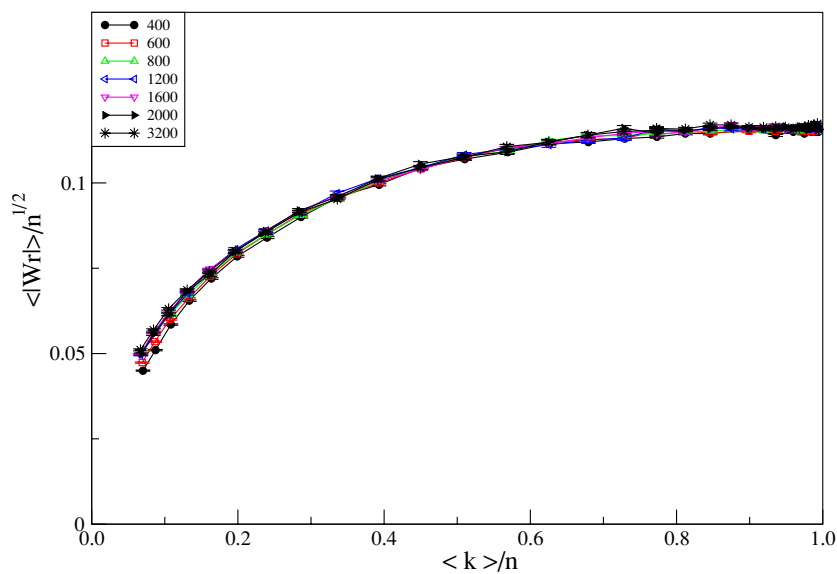


**Figure 4.** The mean of the absolute value of the writhe scaled by  $n^{1/2}$ , as a function of  $\langle k \rangle/n$  for different values of  $n$ .

We have investigated how the knot probability depends on stiffness fugacity and given a semiquantitative argument for the observed behaviour. There is a characteristic stiffness fugacity which maximizes the knot probability and the value of this parameter is not strongly dependent on  $n$ . We have also investigated how the relative probability of the polygon being a trefoil ( $3_1$ ) or figure eight knot ( $4_1$ ) depends on stiffness fugacity and length. We computed

the writhe as a function of stiffness fugacity and found that the expectation of the absolute value of the writhe scales in a similar way for  $\gamma \neq 0$  as for  $\gamma = 0$ .

### Acknowledgment

The authors would like to thank NSERC for financial support.

### References

- [1] Wasserman S A, Dungan J M and Cozzarelli N R 1985 *Science* **229** 171–4
- [2] Wasserman S A and Cozzarelli N R 1986 *Science* **232** 951–60
- [3] Vazquez M and Sumners D W 2004 *Math. Proc. Camb. Phil. Soc.* **136** 565–82
- [4] Edwards S F 1968 *J. Phys. A: Gen. Phys.* **1** 15–28
- [5] Sumners D W and Whittington S G 1988 *J. Phys. A: Math. Gen.* **21** 1689–94
- [6] Pippenger N 1989 *Discrete Appl. Math.* **25** 273–8
- [7] Diaio Y N 1995 *J. Knot Theory Ramifications* **4** 189–96
- [8] Janse van Rensburg E J and Whittington S G 1990 *J. Phys. A: Math. Gen.* **23** 3573–90
- [9] Deguchi T and Tsurusaki K 1997 *Phys. Rev. E* **55** 6245–8
- [10] Yao A, Matsuda H, Tsukuhara H, Shimamura M K and Deguchi T 2001 *J. Phys. A: Math. Gen.* **34** 7563–77
- [11] Orlandini E and Tesi M C 1998 *J. Phys. A: Math. Gen.* **31** 9441–54
- [12] Madras N, Orlitsky A and Shepp L A 1990 *J. Stat. Phys.* **58** 159–83
- [13] Geyer C J 1991 Markov chain Monte Carlo maximum likelihood *Computing Science and Statistics: Proc. 23rd Symp. on the Interface* ed E M Keramidis (Fairfax Station, VA: Interface Foundation) pp 156–63
- [14] Tesi M C, Janse van Rensburg E J, Orlandini E and Whittington S G 1996 *J. Stat. Phys.* **82** 155–81
- [15] Orlandini E 1998 Monte Carlo study of polymer systems by multiple Markov chain method *Numerical Methods for Polymeric Systems* ed S G Whittington (New York: Springer)
- [16] Madras N and Sokal A D 1988 *J. Stat. Phys.* **50** 109–86
- [17] Vologodskii A V, Lukashin A V, Frank-Kamenetskii M D and Anshelevich V V 1974 *Sov. Phys.—JETP* **39** 1059
- [18] Janse van Rensburg E J, Orlandini E, Sumners D W, Tesi M C and Whittington S G 1993 *J. Phys. A: Math. Gen.* **26** L981–6
- [19] Janse van Rensburg E J 2000 *Statistical Mechanics of Interacting Walks, Polygons, Animals and Vesicles* (Oxford: Oxford University Press)